REGULAR ARTICLE

blood advances

Identifying CD38^{+} cells in patients with multiple myeloma: first-in-human imaging using copper-64–labeled daratumumab

Amrita Krishnan,[1,*] Vikram Adhikarla,[2,*] Erasmus K. Poku,[3] Joycelynne Palmer,[2,4] Ammar Chaudhry,[5] Van Eric Biglang-awa,[3] Nicole Bowles,[3] Nitya Nathwani,[1] Michael Rosenzweig,[1] Firoozeh Sahebi,[1,6] Chatchada Karanes,[1] Jennifer Simpson,[7] James F. Sanchez,[1] Dave Yamauchi,[3] Maria Parayno,[3] Arnab Chowdhury,[2] Enrico Caserta,[1,8] Guido Marcucci,[8] Russell Rockne,[2] Anna M. Wu,[9] Jeffrey Wong,[10] Stephen J. Forman,[4] David Colcher,[11] Paul Yazaki,[9] John Shively,[9] and Flavia Pichiorri[1,8]

[1]The Judy and Bernard Briskin Center for Multiple Myeloma Research, [2]Division of Mathematical Oncology, Department of Computational and Quantitative Medicine, Beckman Research Institute, [3]Department of Radiopharmacy, [4]Department of Hematology/Hematopoietic Cell Transplantation, and [5]Department of Diagnostic Radiology, City of Hope, Duarte, CA; [6]Southern California Permanente Medical Group, Los Angeles, CA; and [7]Clinical Trials Office, [8]Department of Hematological Malignancies Translational Science, [9]Department of Molecular Imaging and Therapy, [10]Department of Radiation Oncology, and [11]Department of Molecular Imaging and Therapy, City of Hope, Duarte, CA

Key Points

- In a phase 1 trial, PET/CT imaging using ^{64}Cu–labeled daratumumab was safe and feasible.
- ^{64}Cu-daratumumab localizes to sites of myeloma involvement and may yield favorable sensitivity and specificity.

^{18}F-Fluorodeoxyglucose (FDG) positron emission tomography/computed tomography (PET/CT) is one of the most widely used imaging techniques to detect multiple myeloma (MM). Intracellular FDG uptake depicts in vivo metabolic activity, which can be seen in both malignant and nonmalignant cells, resulting in limited sensitivity and specificity. Our group showed preclinically that tracing MM dissemination using a CD38-directed human antibody, daratumumab, that is radioconjugated with ^{64}Cu via the chelator DOTA (^{64}Cu-daratumumab), led to improved sensitivity and specificity over that of FDG. Here, we report the results of a phase 1 trial designed to (1) assess the safety and feasibility of ^{64}Cu-daratumumab PET/CT and (2) preliminarily evaluate and characterize the ability of ^{64}Cu-daratumumab to accurately detect or exclude MM lesions. A total of 12 daratumumab-naive patients were imaged. Prior to the injection of 15 mCi/5 mg of ^{64}Cu-daratumumab, patients were treated with 0 (n = 3), 10 (n = 3), 45 (n = 3), or 95 mg (n = 3) of unlabeled daratumumab to assess its effect on image quality. No significant adverse events were observed from either unlabeled daratumumab or ^{64}Cu-daratumumab. Of the dose levels tested, 45 mg unlabeled daratumumab was the most optimal in terms of removing background signal without saturating target sites. ^{64}Cu-daratumumab PET/CT provided safe whole-body imaging of MM. A trial comparing the sensitivity and specificity of ^{64}Cu-daratumumab PET/CT with that of FDG PET/CT is planned. This trial was registered at www.clinicaltrials.gov as #NCT03311828.

Introduction

Survival from multiple myeloma (MM) has improved over the past decade in large part because of therapeutic agents such as proteasome inhibitors, immunomodulatory agents, antibody therapy, and high-dose chemotherapy. These advances have led to high response rates and deep responses, including the achievement of minimal residual disease (MRD). Unfortunately, the majority of patients, including those who are MRD-negative, eventually relapse. It is postulated that relapse is due to residual myeloma in the patient, often not detected even with sensitive bone marrow (BM)–based techniques such as multicolor flow cytometry or polymerase chain reaction–based assays. The International

Submitted 8 June 2020; accepted 27 August 2020; published online 23 October 2020. DOI 10.1182/bloodadvances.2020002603.

*A.K. and V.A. contributed equally to this study.

Presented in part at the 2019 Annual Meeting of The American Society of Clinical Oncology, Orlando, FL, 17-20 December 2019.

Requests for data may be made by contacting the corresponding authors, Amrita Krishnan or Flavia Pichiorri, at akrishnan@coh.org or fpichiorri@coh.org.

The full-text version of this article contains a data supplement.

Table 1. Patient characteristics

No.	Sex/age, y	BM involvement by biopsy or aspirate, %	Disease status	R-ISS	Prior radiotherapy	Previous therapy	Dose of unlabeled Dara, mg
1	Male/59	25	Newly diagnosed	Stage II	Yes		0
2	Male/70	6	Relapse by PET	Unknown	No	RVD, autologous stem cell transplantation; lenalidomide maintenance	0
3	Male/69	1	Relapse in pleural lesion by PET	Stage III	Yes	RVD; pomalidomide, daratumumab, dexamethasone; autologous stem cell transplantation	0
4	Male/62	6.4	Relapse by minimal positive PET	Stage I	No	RVD	10
5	Female/52	2	Relapse by PET: diffuse widespread lytic lesions	Stage II	No	RVD	10
6	Female/55	5	Biochemical relapse	Stage I	No	RVD; autologous stem cell transplantation	10
7	Female/55	60	Newly diagnosed	Stage I	No		45
8	Female/64	60	Newly diagnosed	Stage II	No		45
9	Male/67	0	Recurrent plasmacytoma	Unknown	Yes		45
10	Female/61	40	Newly diagnosed	Stage I	No		95
11	Male/72	0	Suspicion of relapse as detected by MRI	Stage III	No	RVD; autologous stem cell transplantation; carfilzomib, lenalidomide, dexamethasone; daratumumab, lenalidomide	95
12	Female/78	40	Newly diagnosed		No		95

MRI, magnetic resonance imaging; RVD, lenalidomide/bortezomib/dexamethasone.

Myeloma Working Group has recognized that marrow involvement in myeloma can be heterogeneous and that true MRD assessment in part depends on imaging.[1] Positron emission tomography/computed tomography (PET/CT) using ^{18}F-fluorodeoxyglucose (^{18}F-FDG) is a widely used imaging technique in MM as a noninvasive disease detection and monitoring strategy, and it is currently the only standardized PET tracer, in particular, with respect to response evaluation.[2] ^{18}F-FDG is a radioactive glucose analog and is taken up by cells with high metabolic activity, a hallmark of cancer cells. It is widely available and does not require local production, making it one of the most commonly used radiotracers. The importance of PET/CT imaging as an essential prognostic factor in MM is highlighted by the finding that in newly diagnosed patients the presence of more than 3 ^{18}F-FDG-positive focal lesions are predictors of poor prognosis,[3] whereas posttreatment PET-negativity alone or combined with a negative MRD signal (ie, flow cytometry or polymerase chain reaction–based sequencing) strongly correlates with better progression-free survival.[3-6] However, ^{18}F-FDG PET/CT has limitations, in regard to both false positives due to infection and inflammation and false negatives associated with concomitant conditions, such as hyperglycemia, recent use of steroids, or very small lesions. Moreover, ^{18}F-FDG uptake may be absent in patients expressing low levels of hexokinase 2 in myeloma cells.[7]

In addition, although myeloma dissemination in the BM, defined as the number of BM lesions, has a prognostic significance when assessed by magnetic resonance imaging,[8] the pattern of marrow infiltration (focal or diffuse) does not necessarily equate with a need for immediate therapy and often is not associated with the presence of bone lesions. Given these limitations and the lack of a well-established alternative, the International Myeloma Working Group has stated that "identification of potentially more sensitive tracers that could overcome the limitations of FDG would be of great interest."[9]

The monoclonal antibody daratumumab binds with high affinity to a unique epitope on CD38, a transmembrane glycoprotein that is highly and ubiquitously expressed on MM cells and at low levels on normal lymphoid and myeloid cells.[10] Given its specificity for plasma cells, as well as our data showing that MM cells maintain higher CD38 levels compared with that in other immune subsets,[11,12] it is an attractive agent for use in imaging in myeloma. We chose ^{64}Cu as a radionuclide because of its suitable half-life (12.7 hours) for preparation and imaging along with the lack of tendency to accumulate in the bones. Our group showed that tracing MM dissemination in a preclinical model using daratumumab radioconjugated with ^{64}Cu via the chelator DOTA (^{64}Cu-daratumumab) led to improved sensitivity and specificity over that of ^{18}F-FDG PET/CT.[13] Moreover, recently published clinical data using ^{89}Zr–labeled daratumumab showed visualization of the agent in the skeleton, liver, and spleen, but the specificity of the myeloma targeting has not been unequivocally verified.[14] Here, for the first time, we are reporting the data of a ^{64}Cu-daratumumab dose-escalation phase 1 imaging trial, which was designed to establish the dose of unlabeled daratumumab that in combination with ^{64}Cu-daratumumab would be safe and optimal to increase MM targeting resolution. Also, as preliminary evidence, we used biopsies to detect the presence or absence of MM cells in regions where ^{18}F-FDG and ^{64}Cu-daratumumab signaling were either concordant or discordant.

Methods

Phase 1 study design and patient population

Between January 2018 and January 2020, a total of 12 patients were enrolled. Subject characteristics are described in Table 1. Our research was approved by our Institutional Review Board. All subjects gave written informed consent. Patients over 18 years of age with histologically confirmed myeloma (either newly diagnosed or relapsed disease), smoldering myeloma, or a solitary plasmacytoma

were eligible. All participants had standard ^{18}F-FDG PET/CT imaging within 60 days of registration but were not required to have measurable or detectable disease by standard PET. Adequate organ function defined as platelet count >50/mm^3, absolute neutrophil acount >1000/mm^3, and bilirubin <1.5 × upper limit of normal was required. The major exclusion criterion was daratumumab therapy within 3 months of enrollment. A total of 12 patients divided into 4 different cohorts (n = 3 for each cohort) were imaged.

Drug administration

Unlabeled daratumumab was IV administered, followed by injection of ^{64}Cu-daratumumab through either a peripheral or a central vein. Standard premedication for daratumumab was administered. Within 6 hours of unlabeled daratumumab administration, patients received 13.63 to 16.68 mCi of ^{64}Cu-daratumumab (~5 mg). Prior to the injection of ^{64}Cu-daratumumab, patients were treated with 0 (cohort 1, n = 3), 10 (cohort 2, n = 3), 45 (cohort 3, n = 3), or 95 mg (cohort 4, n = 3) of unlabeled daratumumab to assess its effect on image quality. The schematic workflow of the trial design is reported in supplemental Figure 1.

PET/CT assessment

Imaging was performed on a GE Discovery STE PET/CT scanner (axial field of view, 15.4 cm). PET images were performed in 3-dimensional mode (septa retracted) and corrected for tissue attenuation on the basis of coregistered CT acquired during the same examination. Attenuation and scatter-corrected PET images were reconstructed on a 128 × 128 matrix with a voxel resolution of 5.5 × 5.5 × 3.3 mm using Ordered Subset Expectation Maximization algorithm with 2 iterations and 20 subsets.

After injection of 15 mCi/5 mg of ^{64}Cu-daratumumab on day 0, scans were performed on days 1 and 2. Because of the limited amount of activity to be injected and the fact that only 18% of ^{64}Cu decays produce a positron, the count rates were expected to be low. To compensate, time per bed position was relatively long. Day 1 scans were acquired at 15 minutes per bed from the top of the head to thighs, while legs were scanned at 10 minutes per bed. On day 2, the time per bed was varied between 15 and 30 minutes within the area of interest, which was typically from the head to the pelvis.

Analysis of the imaged PET/CT data was performed on a GE AW Server. ^{64}Cu-daratumumab standardized uptake values (SUVs) were evaluated as SUV_{mean} and SUV_{max} in organs showing radiotracer uptake. Organ segmentation was performed using the threshold tool on the PET image data while matching the corresponding CT volume. For the BM uptake quantification, the lumbar vertebrae (L1-L5) were evaluated. A 50% SUV_{max} threshold was used to generate the volumes of interest (VOIs). Generated VOIs were manually edited to ensure that the VOI conformed to the vertebral marrow as seen on the CT. Because specific activity in the BM cells and the activity in blood contribute to vertebral uptake measurement, the background activity from blood was estimated to evaluate specific uptake. Briefly, SUV_{mean} of the blood ($SUV_{mean\text{-}blood}$) was measured by placing a VOI in the heart cavity. Using a red marrow to blood concentration ratio of 0.36,[15] the blood contribution to the BM uptake was determined as $\frac{36\ SUV_{mean-blood}}{SUV_{mean-BM}}$ %.

Pharmacokinetic analysis and radiation dosimetry

For subjects given >0 mg of unlabeled daratumumab, blood for pharmacokinetic analysis was drawn at ~15 minutes, 30 minutes, 3 hours, 24 hours, and 48 hours after the end of infusion. Aliquots of whole blood and serum were counted on a gamma counter (Hidex AMG), and the percentage of injected activity in the circulation was calculated.

Imaging-based dosimetry was performed using the SUV_{mean} quantified in the liver, spleen, heart, and the lumbar vertebrae on day 1 and 2. Activity in each of these organs and the rest of the body was calculated using OLINDA-based standard phantom data. Radiotracer whole-body clearance was assumed to be negligible to maximize organ doses. Monoexponential decay fits to the time activity curves were used to calculate residence times and input to OLINDA, yielding the radiation dose estimates to the standard adult phantoms.

See supplemental Information for drug administration and protocol design details.

Results

Biodistribution of ^{64}Cu-daratumumab in patients with myeloma

To evaluate the natural biodistribution of daratumumab, we administered ^{64}Cu-daratumumab without preinfusion of unlabeled daratumumab in the first cohort of patients (n = 3). We imaged 1 newly diagnosed (patient 1) and 2 relapsed MM patients (patients 2 and 3) (Figure 1A; Table 1). Although in all 3 patients we generally detected highly diffuse ^{64}Cu-daratumumab uptake in the spine, pelvis, liver, and spleen (Figure 1A-B), in patient 1 we observed a decrease in radiotracer uptake in the lower cervical spine (C7 SUV_{max} 5.9) compared with that in the lumbar spine vertebrae (L1 SUV_{max} 21.2) (Figure 1A-B top panel). Interestingly, this region of decreased uptake was the site of previously administered involved field radiation (Figure 1A-B). A relatively symmetric pelvic uptake was observed in all 3 patients (Figure 1C), with the exception of the right pelvic area (acetabulum) of patient 3, which was again identified as the site of involved field radiation (Figure 1C bottom panel).

Imaging optimization by infusion of unlabeled daratumumab

We investigated whether normal organ uptake interferes with MM-specific biodistribution of ^{64}Cu-daratumumab. Hence, we proceeded with a dose escalation design using an increased amount (10, 45, and 95 mg) of unlabeled daratumumab before ^{64}Cu-daratumumab infusion. In the cohort of patients pretreated with 10 mg of unlabeled daratumumab and then given ^{64}Cu-daratumumab, we observed reduced radiotracer uptake in the liver (L-SUV_{mean} 11.7 ± 4.0) and spleen (S-SUV_{mean} 23.6 ± 3.7), and a concomitant increase in BM total uptake (BM-SUV_{mean} 19.2 ± 3.1) by day 2, compared with levels in the first cohort of patients in which the unlabeled antibody was not administered (day 2 SUV_{mean}: L, 16.1 ± 0.6; S, 47.2 ± 16.3; BM, 13.7 ± 1.1) (Figure 2A-B; Table 2).

Moreover, a further noticeable decrease in the liver and spleen SUV_{mean} (SUV_{mean}: L, 6.3 ± 1.9; S, 8.6 ± 2.4) was observed when the third cohort of patients, 2 with MM (patient 7 and patient 8) and

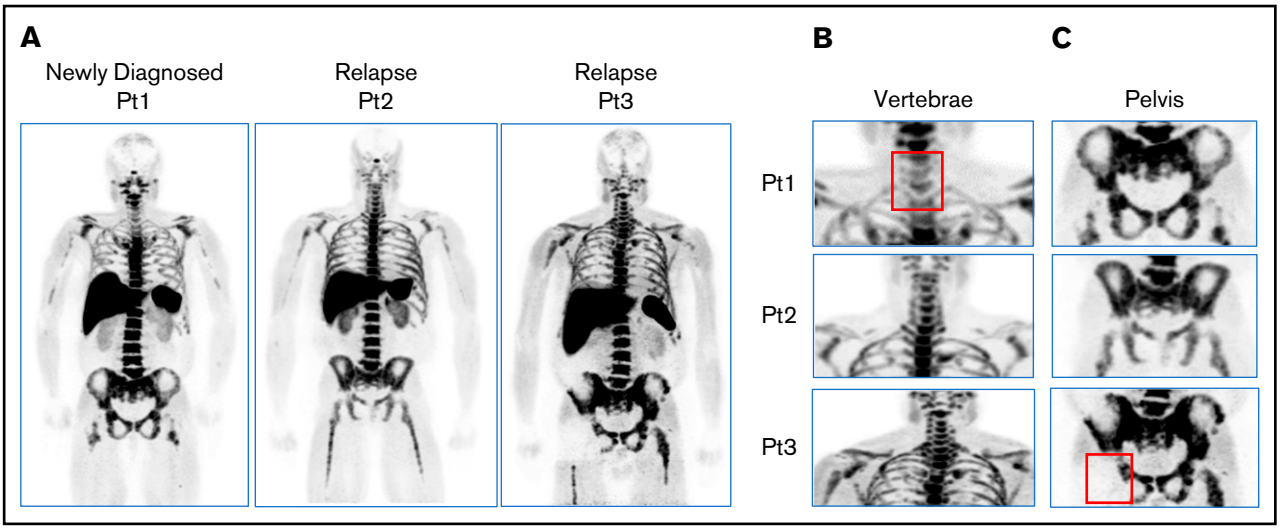

Figure 1. ^{64}Cu-daratumumab biodistribution in subjects imaged without preinfusion of unlabeled daratumumab. (A) Maximum intensity projections showing diffuse ^{64}Cu-daratumumab uptake in the liver, spleen, spine, and pelvis among the 3 patients. Magnification of the cervical (B) and pelvic (C) regions showing reduced radiotracer uptake (red squares) in regions corresponding to the sites in which patient 1 and patient 3 received palliative radiation. pts, patients.

one with a solitary plasmacytoma (patient 9), was pretreated with 45 mg of unlabeled antibody (Figure 2A-B; Table 2). Although the 45-mg cohort clearly showed a decrease in the liver and spleen (SUV_{mean}: L, 6.3 ± 1.9; S, 8.6 ± 2.4), an almost twofold increase in BM SUV_{mean} in patients 7 and 8 was observed (BM-SUV_{mean} 33.9 ± 11.0) over that in the patients given no unlabeled daratumumab (BM-SUV_{mean}: 13.7 ± 1.1) (Table 2). Of note, the ^{64}Cu-daratumumab distribution in the BM of the patient with solitary plasmacytoma showed a completely divergent pattern compared with that observed in the patients with systemic MM (Table 3) and is further discussed below. Finally, when the dose of unlabeled daratumumab was raised to 95 mg, minimal uptake was observed in any of the organs (Figure 2A-B).

The first cohort of patients exhibited rapid clearance of the radiotracer from the bloodstream, indicating that the antibody was preferentially retained by $CD38^+$ cells in the BM, rather than circulating $CD38^+$ cells. A general trend of gradual increase in circulating radiotracer antibody was observed with increased amount of unlabeled daratumumab at early time points (1 to 3 hours) (Figure 2C; supplemental Figure 2). However, this effect was not observed at the 24-hour time point, at which only the patient with a plasmacytoma and the fourth cohort of MM patients (95 mg) maintained high levels of circulating radiotracer (Figure 1C), supporting that the unlabeled daratumumab may had saturated $CD38^+$ cells in the organs of these patients, as well as BM MM cells. As evidence of this saturation, a significant increase in circulating ^{64}Cu-daratumumab was observed in the 95-mg cohort of patients at both early ($P = .013$) and late ($P = .005$) time points over that in the other cohorts (Figure 2C).

For the first 3 cohorts, the background radioactivity from the blood was found to contribute <5% of the radioactivity measured in the BM (Table 3). This finding indicates that most of the radiotracer measured in the BM was specifically bound to cells within the BM. The saturation of the receptors in the BM in patients infused with 95-mg cold antibody was evident, with roughly 42% and 23% of the BM activity attributed to blood-based background signal by day 1 and day 2, respectively.

^{64}Cu-daratumumab accumulates in sites of myeloma involvement

We further investigated the distribution of the radiotracer in the cohort given 45 mg unlabeled daratumumab by comparing uptake in the patients with systemic MM (n = 2) with that in the patient with a solitary plasmacytoma. In the patients with systemic MM, we observed a diffuse uptake of ^{64}Cu-daratumumab throughout the spine (Figure 3A) and a more heterogeneous uptake in the pelvis area, the ribs, and the extremities (Figure 3A-B). Asymmetric focal uptake was observed in the ribs of 1 patient and in the calvarium of both MM patients (Figure 3B). Interestingly, although the 45-mg dose of unlabeled daratumumab also reduced liver and spleen uptake in the patient with a plasmacytoma, as expected, the BM uptake was substantially reduced (day 2 BM-SUV_{mean} 8.4 ± 2.2 vs MM BM-SUV_{mean} 33.9 ± 11.0) (Figure 3B-C; Table 3), an effect we believe is aligned with the absence of MM BM involvement in this patient and with the possible saturation of all CD38 sites by the unlabeled daratumumab. Consistent with this hypothesis, we also did not observe ^{64}Cu-daratumumab uptake in the vertebral plasmacytoma, which underwent biopsy and was shown to be $CD138^+$ and $CD38^+$ by immunohistochemistry (supplemental Figure 3). Indeed, the level of radiotracer in the blood of the patient with a plasmacytoma was comparable to levels found in the cohort receiving a saturating dose of 95 mg unlabeled daratumumab and was higher than the levels in the other patients given the 45-mg dose (Figure 2C), further supporting that the 45-mg unlabeled dose, in the absence of MM BM involvement, may saturate many $CD38^+$ sites. Consistent with these results, the radioactivity in the blood contributing as a background signal to the BM was only ~1% (Table 3) in patients 7 and 8 with MM. Background contribution to the BM from the blood radioactivity was ~12% on day 2 for the patient with plasmacytoma.

Comparison of ^{64}Cu-daratumumab PET/CT with ^{18}F-FDG PET/CT

We compared ^{64}Cu-daratumumab vs ^{18}F-FDG biodistributions generated by our data, and, when possible, performed biopsies in

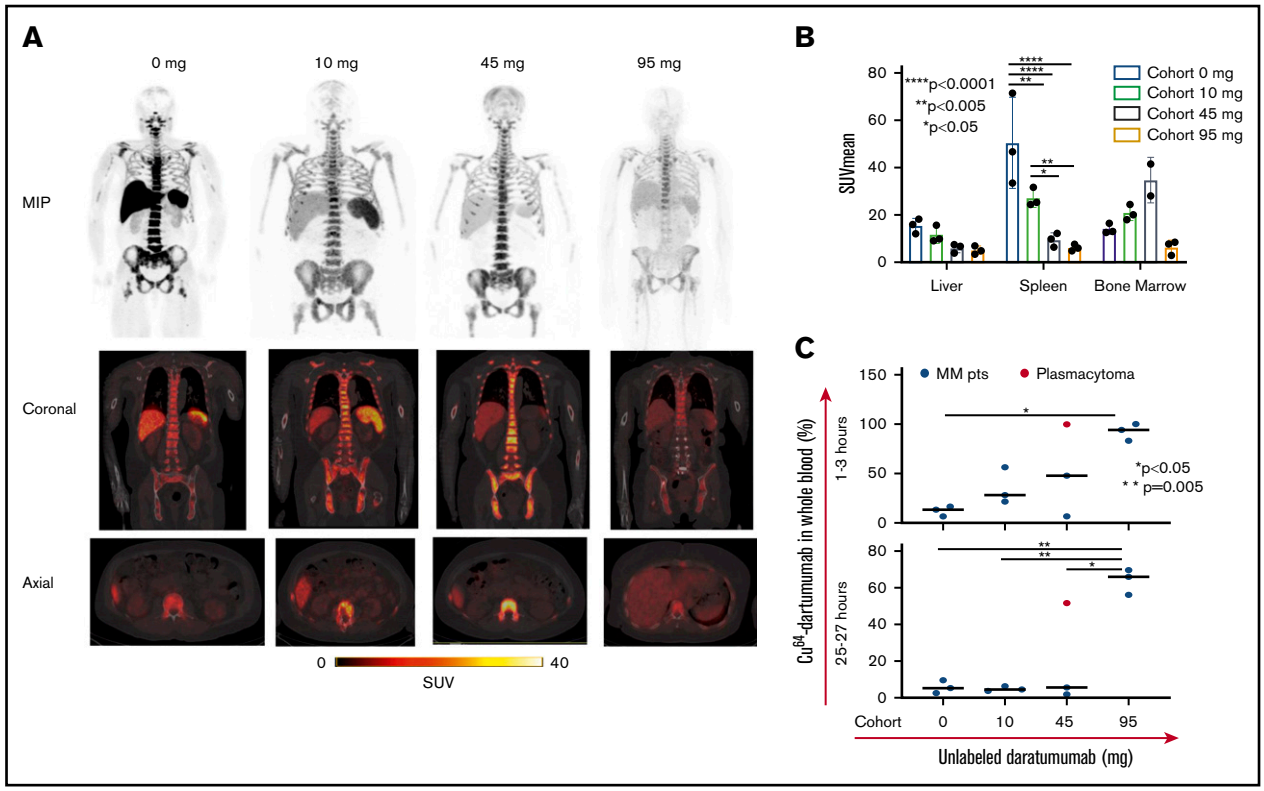

Figure 2. ^{64}Cu-daratumumab uptake as a result of increasing doses of unlabeled daratumumab. (A) PET/CT scan of 1 representative patient from each cohort treated with ^{64}Cu-daratumumab and increasing concentrations of preinfused unlabeled antibody (0, 10, 45, and 95 mg) showing higher liver and spleen uptake in patients who did not receive any unlabeled daratumumab (0 mg) compared with the 10-, 45-, and 95-mg cohort of patients. Increased BM uptake was instead observed in the 10- and 45-mg cohort compared with both the 0- and the 95-mg cohorts. Coronal and axial images through these PET scans are also shown for visualizing relative organ uptake between the cohorts. Color bar is shared between all coronal and axial images. (B) Bar graphs showing the SUV_{mean} values for each cohort in the organs of interest. The BM uptake of the plasmacytoma patient in the 45-mg cohort was not included in the graph. Two-way analysis of variance Tukey multiple comparison test was used to calculate the significance in liver and spleen uptake among treatment cohorts. (C) Dot plots showing radiotracer concentration in the whole blood of the different cohorts at early (1 to 3 hours) and late time points (25 to 27 hours). One-way analysis of variance Tukey multicomparison test was conducted. MIP, maximum intensity projection.

areas in which we found discordant results between these 2 tracers. In general, higher spinal, pelvic, and femoral uptake of ^{64}Cu-daratumumab compared with that of ^{18}F-FDG was observed in all the patients analyzed.

Specifically, patient 1 (newly diagnosed) showed extensive uptake of both tracers (Figure 4A), and comparable focal uptake between the 2 was observed in the right and left humerus (Figure 4A). We also observed a diffuse uptake of ^{64}Cu-daratumumab in the pelvis and a more focal uptake in the femoral bones and legs (patient 7), but no specific ^{18}F-FDG signals were observed in these areas (Figure 4A-B). A concordant positive signal (SUV_{max} of 14.7 on ^{64}Cu-daratumumab PET/CT vs 3.3 on ^{18}F-FDG PET/CT) was also observed in the sternum of patient 1, a site that was confirmed positive for myeloma infiltration by biopsy (Figure 4C). In the iliac crest region of the same patient, we noted no ^{18}F-FDG signal but observed ^{64}Cu-daratumumab uptake; this site was found to be positive for myeloma by biopsy (20% to 30% CD138^{+} MM plasma

Table 2. ^{64}Cu-daratumumab (SUV_{mean}) uptake and background contribution of blood activity to BM uptake categorized by dose of unlabeled daratumumab

	0 mg		10 mg		45 mg		95 mg	
Organs	**Day 1**	**Day 2**	**Day 1**	**Day 2**	**Day 1**	**Day 2**	**Day 1**	**Day 2**
BM	14.1 ± 2.1	13.7 ± 1.1	20.9 ± 3.3	19.2 ± 3.1	34.8 ± 9.6*	33.9 ± 11.0*	6.4 ± 3.0	7.3 ± 3.8
Liver	15.5 ± 3.1	16.1 ± 0.6	11.6 ± 3.5	11.7 ± 4.0	6.1 ± 1.9	6.3 ± 1.9	5.1 ± 1.8	5.0 ± 1.7
Spleen	50.5 ± 19.3	47.2 ± 16.3	27.2 ± 4.0	23.6 ± 3.7	9.5 ± 2.9	8.6 ± 2.4	6.2 ± 1.4	5.5 ± 1.5
Blood (heart)	1.8 ± 0.6	1.3 ± 0.6	1.5 ± 0.1	1.5 ± 0.4	0.9 ± 0.3*	0.8 ± 0.4*	7.5 ± 0.3	4.6 ± 0.9
Blood activity contribution to BM, %	4.7 ± 1.6	3.4 ± 1.6	2.6 ± 0.4	2.9 ± 0.9	1.0 ± 0.4*	0.9 ± 0.5*	42.0 ± 19.8	22.7 ± 12.6

*Average of the 2 newly diagnosed MM patients (patient 7 and patient 8).

Table 3. Organ uptake (SUV_{mean}) and background contribution of blood activity to BM uptake in patients at 45-mg cold dose of daratumumab

	MM patients (patient 7, patient 8)		Solitary plasmacytoma patient (patient 9)	
Organs	**Day 1**	**Day 2**	**Day 1**	**Day 2**
Lumbar vertebrae	34.8 ± 9.6	33.9 ± 11.0	7.4 ± 1.6	8.4 ± 2.2
Liver	5.7 ± 2.6	6.0 ± 2.5	6.8 ± 1.1	7.1 ± 1.6
Spleen	9.3 ± 4.1	8.4 ± 3.6	9.8 ± 1.6	9.0 ± 1.9
Blood (heart)	0.9 ± 0.3	0.8 ± 0.4	4.6 ± 0.8	2.7 ± 0.8
Blood activity contribution to BM, %	1.0 ± 0.4	0.9 ± 0.5	22.5 ± 7.3	11.5 ± 5.1

cells) (Figure 4C). Discordant uptake of the 2 tracers in the iliac crest was also observed in patient 8. The iliac crest of this patient was also positive by ^{64}Cu-daratumumab imaging and by biopsy (60% plasma cell infiltration), but negative by ^{18}F-FDG (Figure 4D). Conversely, in another patient (patient 2), we observed positive uptake of ^{18}F-FDG in the right clavicular region that instead was negative according to both ^{64}Cu-daratumumab signal and biopsy (Figure 4E). In patient 3, a positive signal by ^{18}F-FDG PET/CT was seen in a pleural-based mass, with an SUV_{max} of 9.0. In contrast, this region did not show specific uptake of ^{64}Cu-daratumumab and was negative by biopsy, suggesting that the ^{18}F-FDG uptake was a false positive (Figure 4F). Furthermore, focal ^{64}Cu-daratumumab uptake in the calvarium was observed in 8 out of 12 MM patients analyzed, and in patient 1, the focal uptake was mainly localized around calvarium bone lesions (Figure 4G), suggesting that antibody-based imaging may be superior to identify the presence of cancer cells at this site, which may be obscured by high uptake of ^{18}F-FDG in the brain (Figure 4A,C,G).

Radiation dosimetry

Absorbed dose estimates calculated using the data from the third cohort of patients preinfused with 45 mg of cold antibody are shown in supplemental Table 1. Red marrow, spleen, and liver doses were 0.32 ± 0.22, 0.24 ± 0.07, and 0.16 ± 0.06 mSv/MBq, respectively. The whole-body effective dose was 0.07 ± 0.02 mSv/MBq.

Discussion

We have validated our preclinical data that ^{64}Cu-daratumumab PET/CT imaging provides whole-body imaging of MM. In this first-in-human trial, we also demonstrated the safety and potential clinical applications of this immune-PET imaging strategy.

Daratumumab has become a widely used antibody in MM therapy.[16-18] Toxicities are moderate and manageable, the most common being infusion-related toxicities, which are frequently encountered with monoclonal antibodies. Both the amounts of ^{64}Cu-daratumumab (~5 mg) and unlabeled daratumumab (≤95 mg) used in this study are considerably less than the typically prescribed 16-mg/kg dose.

Our data suggest that the 45-mg cold dose may be optimal for myeloma imaging, as liver and spleen uptake were greatly reduced while the marrow uptake was maximized, in contrast to the other cohorts. The higher dose of 95 mg appeared to saturate the CD38 receptors and limit uptake by known sites of disease. This concept

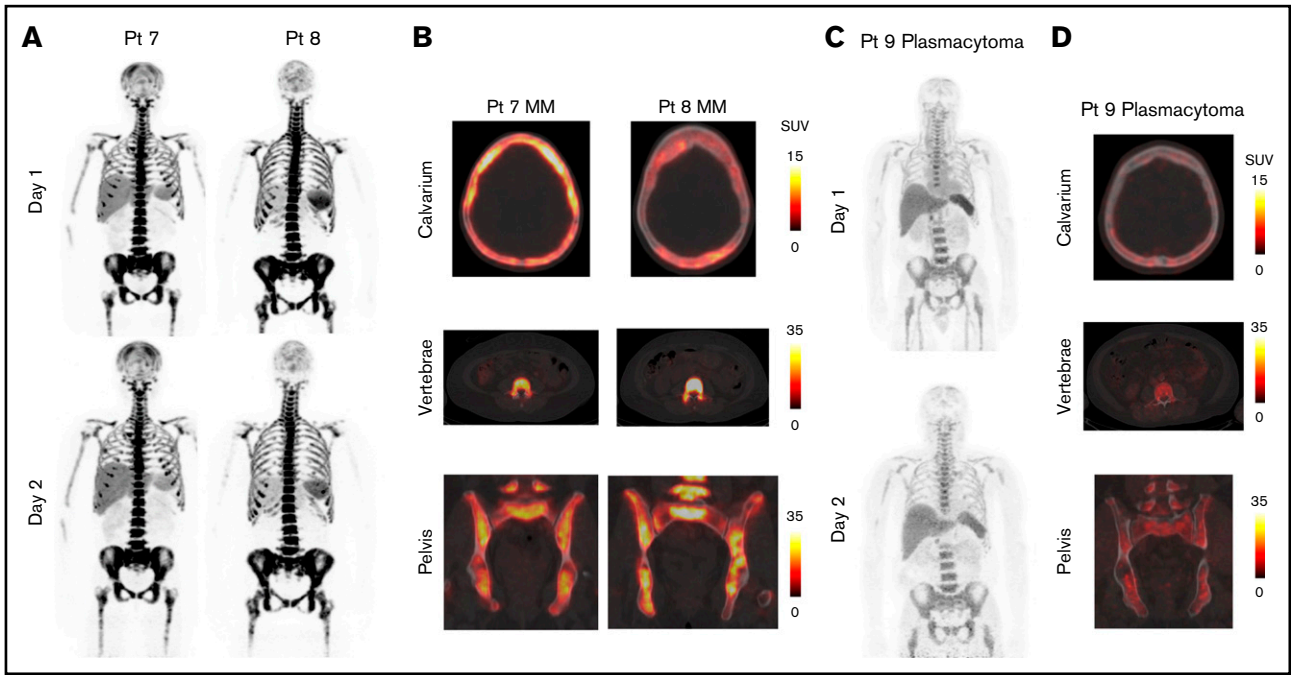

Figure 3. Accumulation of ^{64}Cu-daratumumab in patients preadministered 45 mg of unlabeled daratumumab. (A) Maximum intensity projections on day 1 and day 2 showing significant BM uptake in the 2 patients with systemic MM. (B) Calvarial, vertebral, and pelvic uptake of ^{64}Cu-daratumumab shown in coronal views of the PET/CT fused image. Color bars for the fused PET/CT images are shared between patient 7 and patient 8. (C-D) The patient with a solitary plasmacytoma had comparatively low levels of radiotracer in the marrow and enhanced activity in the circulation, as evident from the day 1 scan. Heterogeneous and elevated uptake of radiotracer in all 3 regions is seen in the first 2 patients when compared with the patient with solitary plasmacytoma.

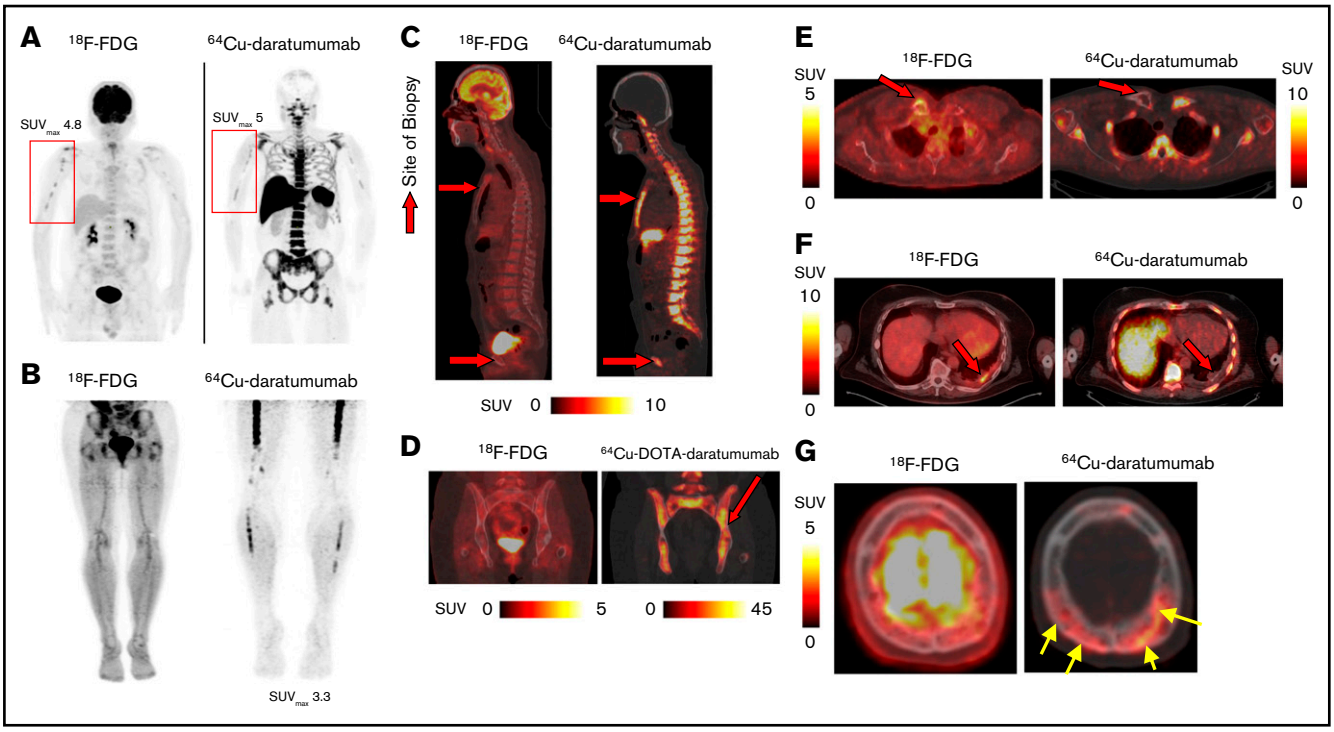

Figure 4. Comparison of ^{64}Cu-daratumumab with ^{18}F-FDG. (A-B) Maximum intensity projections comparing the uptake of ^{64}Cu-daratumumab with ^{18}F-FDG. Similar skeletal uptake in the right humerus for both tracers was observed (red rectangles) in patient 1 (A), while ^{64}Cu-daratumumab, but not ^{18}F-FDG uptake in the femur and fibula (SUV_{max} 3.3), was observed in patient 7 (B). (C) Sagittal cross-section through scans comparing ^{64}Cu-daratumumab and ^{18}F-FDG uptake in 2 regions (sternum and pelvis, red arrows) found positive for MM infiltration by biopsy. (D) Heterogeneous pelvis uptake of ^{64}Cu-daratumumab in the region that was found positive for MM by biopsy (red arrow), but negative by ^{18}F-FDG. (E) Biopsy acquired (red arrow) from patient 2 with right clavicular uptake on ^{18}F-FDG but not on ^{64}Cu-daratumumab, which was negative for MM infiltration upon biopsy. (F) Sagittal cross-section through scans comparing ^{64}Cu-daratumumab and ^{18}F-FDG uptake in another patient showing elevated ^{18}F-FDG and no ^{64}Cu-daratumumab uptake in the pleural-based mass, a region indicated to be myeloma-negative by biopsy. (G) Prominent calvarial uptake (yellow arrows) around bone lesions was seen in the ^{64}Cu-daratumumab PET images of patient 1, which is typically obscured by the brain uptake of ^{18}F-FDG. Color bars are shared between the ^{18}F-FDG PET and ^{64}Cu-DOTA–daratumumab PET images when 1 color bar is grouped with a pair of images.

of receptor saturation is further supported by results with the single patient with a solitary plasmacytoma, in whom a 45-mg cold dose may have exceeded the optimal amount by saturating all target sites.

In addition, this finding may have implications in patients pretreated with daratumumab. Although we have observed that patients who are no longer responding to daratumumab continue to exhibit expression of CD38 on their plasma cells,[11] it is possible that patients with high levels of circulating daratumumab from prior therapy may have receptor saturation at the time of administration of radiolabeled daratumumab. We will explore this aspect further in the phase 2 trial, where we will not exclude patients currently on daratumumab therapy. The study procedures were well tolerated; in 1 patient, we observed grade 3 toxicities of hypoxia and hypertension related to the infusion of unlabeled daratumumab, in keeping with the known side effects of the drug, which was successfully managed with additional diphenhydramine and hydrocortisone. Recently, 1 phase 3 noninferiority trial disclosed that a subcutaneous route of administration leads to significantly lower rates of these reactions (12.7% vs 35%).[19] No serious adverse events were associated with ^{64}Cu-daratumumab.

The design of the immunological imaging agent needs to specifically consider the radionuclide, the chelator, and the antibody. A radionuclide with an appropriate half-life (order of hours to days) is essential. In this regard, both ^{64}Cu ($t_{1/2}$ = 12.7 hours) and ^{89}Zr ($t_{1/2}$ = 78.4 hours) are being explored for imaging MM disease burden, with their half-lives facilitating imaging times up to 2 days and a week, respectively. The advantages of ^{64}Cu-based imaging compared with ^{89}Zr-based imaging include the possibility of administering greater activity for better sensitivity or lowering the radiation dose to the patient for similar imaging results. The longer half-life of ^{89}Zr compared with ^{64}Cu results in an increased radiation dose from ^{89}Zr and typically limits the amount of injected radioactivity for comparable dosimetry. The improved dosimetry of ^{64}Cu over ^{89}Zr becomes especially important with respect to highly specific radiotracer uptake and retention in the BM. Since increased disease burden will result in increased radiotracer accumulation in the BM, the extended retention of radioactivity in the BM results in increased radiation dose. The delayed imaging with ^{89}Zr is advantageous for cases where the signal from disease is significantly hampered by background tissue uptake. In the ^{89}Zr study, imaging 5 to 6 days postradiotracer infusion has been suggested as a potential imaging timeframe on the basis of the femoral uptake and the clearance of activity from the blood. In our trial, we note that the background contribution of the blood radioactivity is a minor part of the activity measured in the BM. Of the 9 patients imaged in the first 3 cohorts, the only case of elevated levels of circulating radiotracer

at the 24-hour time point, as could also be seen on the PET imaging scans, was of the patient with a solitary plasmacytoma, who had the highest blood SUV_{mean} compared with the other patients analyzed. By 48 hours, the presence of the radiotracer was not seen (Figure 3C), a result supported by the much lower activity measured in the blood at day 2 (supplemental Figure 2).

Quantitative evaluation indicated that >95% of the activity measured in the BM was specifically bound and <5% of the activity was attributed to background contribution from blood. This finding implies that ^{64}Cu-daratumumab is rapidly taken up by the BM of patients with MM, leaving little in the blood circulation by 48 hours, supporting rapid elimination of the radiotracer background and feasibility of imaging within the first 2 days of radiotracer infusion.

Although we do not hypothesize that the high BM SUV is an indication of widespread diffuse disease, one can postulate that there is likely more extensive bone and marrow involvement detected by ^{64}Cu-daratumumab imaging than in standard imaging, which will be investigated further.

Our trial is the first of radiolabeled daratumumab imaging to use biopsies to investigate discordances between ^{18}F-FDG PET/CT and ^{64}Cu-daratumumab imaging. We showed that 2 lesions that were ^{18}F-FDG positive but ^{64}Cu-daratumumab negative did not have evidence of MM by tissue biopsy and instead had evidence of an inflammatory reaction. Although we cannot exclude a heterogeneous distribution of myeloma being responsible for the failure to detect disease by biopsy, these patients did not progress in the regions where these biopsies occurred upon clinical follow-up. We also demonstrated that lesions that were ^{18}F-FDG negative but ^{64}Cu-daratumumab positive were positive for myeloma involvement on biopsy. Also of note was the skull uptake: since there was no brain uptake of ^{64}Cu-daratumumab in contrast to standard ^{18}F-FDG, we were able to demonstrate focal calvarial uptake, which allows better evaluation of skull plasmacytomas. These findings lay the groundwork for a phase 2 trial comparing the sensitivity and specificity of both imaging strategies. A key disadvantage in general of antibody-based imaging is the extended time for which the patient needs to be scanned compared with ^{18}F-FDG PET. ^{18}F-FDG PET scans are typically acquired at 2 to 3 minutes per bed position. ^{64}Cu-DOTA–daratumumab PET scans in this trial were acquired between 10 and 30 minutes per bed position on the Discovery STE PET/CT scanner to maximize the imaging signal. Given the high SUVs measured in patient BM, reduction in scan time can be explored in the future. Recent developments on whole-body PET scanners[20] would make antibody-based imaging much faster than the current protocols.

If successful, ^{64}Cu-daratumumab PET/CT may be applied in several settings. For smoldering MM, laboratory values, standard imaging methods, and clinical criteria are currently used to differentiate smoldering MM from active MM. However, this area remains in significant flux, as evidenced by the changing definitions of smoldering myeloma.[21,22] It would be of interest to investigate the utility of ^{64}Cu-daratumumab PET/CT in the early detection of disease as a potentially more sensitive imaging modality than standard ^{18}F-FDG PET/CT, which in turn may lead to better selection of patients who could benefit from early therapy. We envision that evaluation of MRD in MM will eventually be supplemented or even replaced by such a molecular imaging modality. Furthermore, ^{64}Cu-DOTA–daratumumab PET/CT may be studied as a potential predictor of response to therapies. A key advantage of using ^{64}Cu-DOTA–daratumumab is the ease of chelation of numerous radionuclides to the DOTA chelator, potentially allowing imaging with ^{64}Cu-DOTA–daratumumab to guide daratumumab-based radiotherapies. Moreover, the possibility of performing imaging at earlier time points may favor a rapid initiation of therapy and facilitate improved patient management.

Acknowledgments

The authors acknowledge support from the Steven Gordon and Briskin Family Innovation Grant and are grateful to Young Kim for assistance with immunohistochemistry. The authors are also grateful for support from Steve Allen, Suzan King, and the Tom Klemens Family Foundation.

The Biostatistics and Mathematical Modeling Core and the GMP Manufacturing Core at City of Hope were supported by the National Institutes of Health, National Cancer Institute under award number P30CA033572. This research was also in part supported by National Institutes of Health, National Cancer Institute NIH-2-R01-CA238429-01 (F.P., J. Shively, and R.R.).

The content is solely the responsibility of the authors and does not necessarily represent the official views of the National Institutes of Health.

Authorship

Contribution: A.K., V.A., J.P., A. Chaudhry, E.C., G.M., R.R., A.M.W., J.W., S.J.F., D.C., P.Y., J. Shively, and F.P. designed research; A.K., V.A., E.K.P., A. Chaudhry, V.E.B.-a., N.B., N.N., M.R., F.S., C.K., and J. Simpson performed research; A.K., V.A., J.P., A. Chaudhry, J.F.S., D.Y., M.P., A. Chowdhury, and F.P. analyzed data; A.K., V.A., J.P., J. Simpson, J.F.S., and F.P. wrote the manuscript; and all authors reviewed the manuscript.

Conflict-of-interest disclosure: A.K. is a consultant for Bristol Myers Squibb, GlaxoSmithKline, Janssen Pharmaceuticals, Karyopharm Therapeutics, and Regeneron Pharmaceuticals; is on the scientific advisory board for Sutro Biopharma; serves on the speakers bureau for Amgen, Bristol Myers Squibb, and Takeda; and has stock ownership in Bristol Myers Squibb. J.P. is a consultant for Gilead. M.R. is on the speakers bureau for Janssen Pharmaceuticals. The remaining authors declare no competing financial interests.

ORCID profiles: A. Chaudhry, 0000-0002-2126-0587; N.N., 0000-0003-4329-8102; J.F.S., 0000-0002-2254-6894; A. Chowdhury, 0000-0003-4683-9242; J. Shively, 0000-0002-7763-770X.

Correspondence: Amrita Krishnan, The Judy and Bernard Briskin Center for Multiple Myeloma Research, City of Hope, 1500 E Duarte Rd, Duarte, CA 91010; e-mail: akrishnan@coh.org; and Flavia Pichiorri, The Judy and Bernard Briskin Center for Multiple Myeloma Research, Department of Hematological Malignancies Translational Science, City of Hope, 1500 E Duarte Rd, Duarte, CA 91010; e-mail: fpichiorri@coh.org.

References

1. Kumar S, Paiva B, Anderson KC, et al. International Myeloma Working Group consensus criteria for response and minimal residual disease assessment in multiple myeloma. *Lancet Oncol*. 2016;17(8):e328-e346.
2. Zamagni E, Nanni C, Dozza L, et al. Standardization of 18F-FDG PET/CT according to Deauville Criteria for MRD evaluation in newly diagnosed transplant eligible multiple myeloma patients: joined analysis of two prospective randomized phase III trials [abstract]. *Blood*. 2018;132(suppl 1). Abstract 257.
3. Zamagni E, Patriarca F, Nanni C, et al. Prognostic relevance of 18-F FDG PET/CT in newly diagnosed multiple myeloma patients treated with up-front autologous transplantation. *Blood*. 2011;118(23):5989-5995.
4. Usmani SZ, Mitchell A, Waheed S, et al. Prognostic implications of serial 18-fluoro-deoxyglucose emission tomography in multiple myeloma treated with total therapy 3. *Blood*. 2013;121(10):1819-1823.
5. Lapa C, Lückerath K, Malzahn U, et al. 18 FDG-PET/CT for prognostic stratification of patients with multiple myeloma relapse after stem cell transplantation. *Oncotarget*. 2014;5(17):7381-7391.
6. Moreau P, Attal M, Caillot D, et al. Prospective evaluation of magnetic resonance imaging and [^{18}F]fluorodeoxyglucose positron emission tomography-computed tomography at diagnosis and before maintenance therapy in symptomatic patients with multiple myeloma included in the IFM/DFCI 2009 trial: results of the IMAJEM study. *J Clin Oncol*. 2017;35(25):2911-2918.
7. Rasche L, Angtuaco E, McDonald JE, et al. Low expression of hexokinase-2 is associated with false-negative FDG-positron emission tomography in multiple myeloma. *Blood*. 2017;130(1):30-34.
8. Walker R, Jones-Jackson L, Rasmussen E, et al. Diagnostic imaging of multiple myeloma-FDG PET and MRI complementary for tracking short vs. long term tumor response [abstract]. *Blood*. 2004;104(11). Abstract 758.
9. Cavo M, Terpos E, Nanni C, et al. Role of ^{18}F-FDG PET/CT in the diagnosis and management of multiple myeloma and other plasma cell disorders: a consensus statement by the International Myeloma Working Group. *Lancet Oncol*. 2017;18(4):e206-e217.
10. Malavasi F, Deaglio S, Funaro A, et al. Evolution and function of the ADP ribosyl cyclase/CD38 gene family in physiology and pathology. *Physiol Rev*. 2008;88(3):841-886.
11. Viola D, Dona A, Caserta E, et al. Daratumumab induces mechanisms of immune activation through CD38+ NK cell targeting [published online ahead of print 16 April 2020]. *Leukemia*. doi:10.1038/s41375-020-0810-4.
12. Ghose J, Viola D, Terrazas C, et al. Daratumumab induces CD38 internalization and impairs myeloma cell adhesion. *OncoImmunology*. 2018;7(10):e1486948.
13. Caserta E, Chea J, Minnix M, et al. Copper 64-labeled daratumumab as a PET/CT imaging tracer for multiple myeloma [published correction appears in *Blood*. 2018;131(25):2869]. *Blood*. 2018;131(7):741-745.
14. Ulaner GA, Sobol NB, O'Donoghue JA, et al. CD38-targeted immuno-PET of multiple myeloma: from xenograft models to first-in-human imaging. *Radiology*. 2020;295(3):606-615.
15. Sgouros G. Bone marrow dosimetry for radioimmunotherapy: theoretical considerations. *J Nucl Med*. 1993;34(4):689-694.
16. Lonial S, Weiss BM, Usmani SZ, et al. Daratumumab monotherapy in patients with treatment-refractory multiple myeloma (SIRIUS): an open-label, randomised, phase 2 trial. *Lancet*. 2016;387(10027):1551-1560.
17. Dimopoulos MA, Oriol A, Nahi H, et al; POLLUX Investigators. Daratumumab, lenalidomide, and dexamethasone for multiple myeloma. *N Engl J Med*. 2016;375(14):1319-1331.
18. Palumbo A, Chanan-Khan A, Weisel K, et al; CASTOR Investigators. Daratumumab, bortezomib, and dexamethasone for multiple myeloma. *N Engl J Med*. 2016;375(8):754-766.
19. Mateos M-V, Nahi H, Legiec W, et al. Efficacy and safety of the randomized, open-label, non-inferiority, phase 3 study of subcutaneous (SC) versus intravenous (IV) daratumumab (DARA) administration in patients (pts) with relapsed or refractory multiple myeloma (RRMM): COLUMBA. *J Clin Oncol*. 2019;37(15 suppl):8005-8006.
20. Cherry SR, Jones T, Karp JS, Qi J, Moses WW, Badawi RD. Total-body PET: maximizing sensitivity to create new opportunities for clinical research and patient care. *J Nucl Med*. 2018;59(1):3-12.
21. Rajkumar SV, Dimopoulos MA, Palumbo A, et al. International Myeloma Working Group updated criteria for the diagnosis of multiple myeloma. *Lancet Oncol*. 2014;15(12):e538-e548.
22. Lakshman A, Rajkumar SV, Buadi FK, et al. Risk stratification of smoldering multiple myeloma incorporating revised IMWG diagnostic criteria. *Blood Cancer J*. 2018;8(6):59.